

Design and predicted performance of the GMT ground-layer adaptive optics mode

Phillip M. Hinz^a, Guido Brusa^a, Vidhya Vaitheeswaran^a, Tom McMahon^a, Tom Connors^a, Russell Knox^a, Antonin Bouchez^b, Manny Montoya^a

^aSteward Observatory, Univ. of Arizona, 933 N. Cherry Ave., Tucson, AZ, USA 85721

^bGMTO Corp., 251 S. Lake Ave., Pasadena, CA, USA 91101;

ABSTRACT

The Giant Magellan Telescope is planning to provide adaptive wavefront correction of the low layers (<1 km) of atmospheric turbulence in support of wide-field instrumentation. This ground-layer adaptive optics (GLAO) mode will use the adaptive secondary mirrors to provide improved image quality over approximately 7 arcminutes FOV. We present a comparison between the use of a sodium laser guide star asterism plus three tip-tilt natural guide stars versus natural guide stars only on the average seeing width improvement. The layout and components of both (laser beacon based and natural star only based) GLAO concepts are described and the impact and interaction with other GMT sub-systems is analyzed.

Keywords: Extremely Large Telescopes, Adaptive Optics, Wavefront Sensing, Tomography, Laser Guidestar

1. INTRODUCTION

The Giant Magellan Telescope (GMT) has an adaptive optics (AO) system well suited for wide-field imaging and spectroscopy. By integrating the wavefront correction into the secondary mirrors, the same focal plane that is available to seeing-limited instruments can be used by AO-assisted instruments. A promising mode for this architecture is ground-layer adaptive optics (GLAO), which aims at correcting the turbulence below approximately 1 km. Such an approach improves image sharpness over a wide field of view. This approach suggests that the design of the GLAO should minimize the impact of its operation on the wide-field instruments that will utilize the system, therefore the effects on throughput, efficiency, and robustness need to be carefully considered in the GLAO system design.

This paper describes the trade-off in performance, cost, and risk of two concepts for a Ground-Layer Adaptive Optics System for the Giant Magellan Telescope. The two concepts being considered are:

- A Laser Guide Star (LGS) based system, using 6 sodium laser beacons, along with 3 natural guide star tip-tilt sensors, this is the LGS Ground Layer Adaptive Optics (LGLAO) option.
- A Natural Guide Star (NGS) based system, using 4 guide stars selected in the annular field around the science field, this is the NGS Ground Layer Adaptive Optics (NGLAO) option.

The two main performance requirements for the GLAO system as stated by the GMTO (see Bouchez et al.¹) are: <0.30 arcsec image FWHM at K band over >6.5 arcmin diameter (SCI-1887) and 15% image FWHM reduction in I band over >6.5 arcmin diameter (SCI-4509), these requirements are specified at 15° from zenith and median atmospheric conditions ($r_0@500\text{nm} = 16.4\text{ cm}$ at zenith).

2. GLAO CONCEPTUAL LAYOUT

The LGLAO and NGLAO options are described in this section to introduce the simulation results and to compare complexity and operation concepts.

2.1 LGS-based Ground-Layer AO Conceptual Design (LGLAO)

When using the LGLAO system measurements from 6 sodium laser guide stars are averaged to produce an estimate of the ground-layer contribution to atmospheric seeing and correct for correlated turbulence closer to the telescope pupil. Correction of the lower layers results in an improved and uniform PSF over a wide FoV.

In addition to the 6 laser system the GMT's laser based GLAO system comprises the adaptive secondary mirrors (ASMs) system, a large dichroic, the 6-Shack-Hartmann WFS system for Laser guide stars beacon sensing, 3 NGS cameras to measure tip-tilt, 1 truth WFS to measure static aberration. The ground layer correction is computed by merging higher order signals from the LGS WFS with tip-tilt signals from the three NGS tip-tilt sensors and the truth sensor. The resulting slope vector is used for WFS reconstruction using a pre-calibrated reconstructor matrix.

2.2 LGLAO Opto-Mechanics

Figure 1 left illustrates the division of light for the LGLAO option: the laser beacon photons returned from the range of 90-100 km reach a large dichroic that reflects the laser light to six Shack-Hartmann sensors on the instrument platform. Shack-Hartmann patterns for each of the six guide stars are sampled on a regular grid of sub apertures (up to 24x24 for the simulation; 40x40 for the conceptual design). To sample the Shack-Hartmann patterns a CCD-220 e2v sensor is operated at a rate of 500 frames per second. The visible light from suitable tip-tilt stars is sent to the tip-tilt sensing system, at the moment for the tip-tilt sensing we are considering using an Andor Xion or similar EMCCD. Because of the large dichroic size the natural stars for tip-tilt measurement have to be outside 8' (radius) from the center of the field.

The truth WFS is a 12×12 Shack-Hartmann sensor that uses an additional natural guide star with a sampling rate of 1-5Hz to sample the static aberration and focus drift left uncorrected by the laser guide star system.

The opto-mechanics for the LGLAO option are comprised of the large dichroic and mount, the GLAO WFS Carriage assembly, and the NGS WFS patrol mechanisms. The dichroic and Carriage assembly are shown in Figure 2.

The dichroic is sized for a 9.2' diameter FoV and at about 1 meter from the focal plane has a diameter of 730 mm. The dichroic plus its assembly block the central 812 mm diameter area which preventing using tip-tilt guide stars inside an $\sim 8'$ radius (the maximum transferred field has a radius of 10').

2.3 LGLAO Technical Challenges

The technical challenges in deploying and operating the LGLAO option fall into several distinct areas. The primary opto-mechanical challenge is the fabrication of the large dichroic. The mounting of the dichroic must be carefully considered to minimize gravity-induced deformation. A second challenge consists in the focal plane shift introduced by the dichroic, the 22 mm shift can be compensated by a secondary mirror piston of 0.16 mm however this puts in approximately 11 μm of peak-to-valley spherical aberration. This amount of spherical aberration can be compensated by the ASM but only by using a significant fraction of the ASM actuator stroke and maximum allowable forces.

A second category of issues is related to the laser beacon projectors. These are shared with the LTAO system however use of the projectors for both LTAO and GLAO requires them to be adjustable from a small ($\sim 1.5'$) LTAO asterism to a large (up to 7' diameter) GLAO asterism.

Finally, there is an operational challenge; the GLAO system is primarily used to improve SNR of observations via image sharpening, thus a high system observation efficiency is required to compete with similar seeing-limited observations. Given the LGLAO system complexity, this high efficiency is considered a challenge particularly in comparison with the much simpler NGLAO system described in the next section.

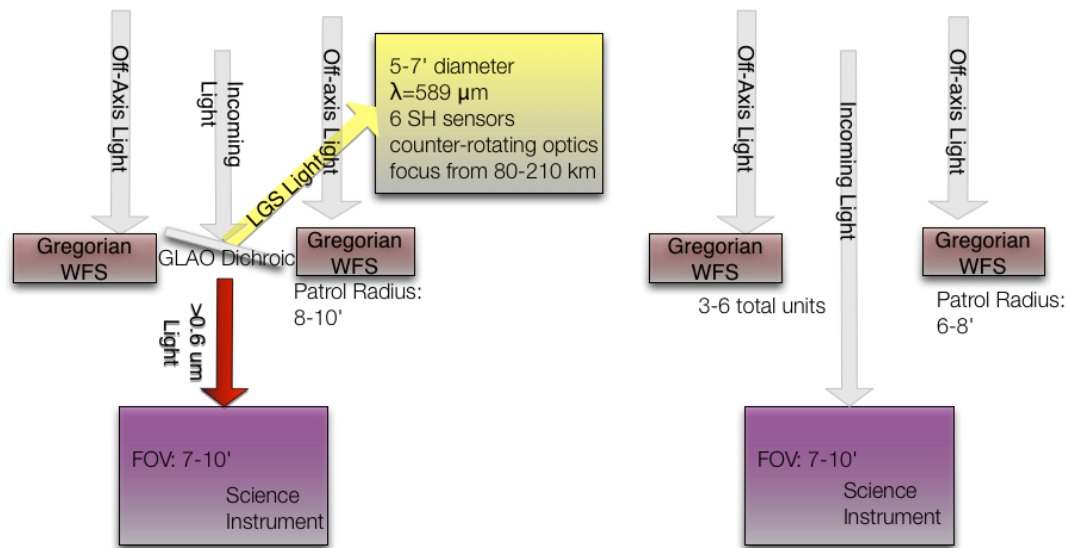


Figure 1 (Left) Conceptual diagram for the GMT LGLAO system, (Right) Conceptual Diagram for the GMT NGLAO system.

2.4 NGS-based Ground-Layer AO Conceptual Design (NGLAO)

The NGLAO option configuration uses 3-6 natural guide stars available in the technical field (annulus) around the central science field (see Figure 1 right). The guide stars are used both for tip-tilt sensing and high-order wavefront sensing.

For the concept considered here, a set of 4 patrolling cameras are located inside the instrument platform. These are envisioned to be the same devices that would be used for active optics and phasing, although the approach to merging these needs is considered to be a task for future studies. Each camera will patrol one quadrant. The implementation of this mode would utilize an AO guide star selection tool that would query standard star catalogs (2MASS, Sloan Digital Sky Survey, GSC, Virtual Observatory etc) to create a list of potential guide stars. The guide star selection tool may be required to cross reference multiple listings of the same star from several catalogs and validate magnitude of the star lists. It is anticipated that this tool would interface with the active optics system to reduce acquisition overheads. The NGLAO will also use turbulence profile knowledge to compute an optimal reconstructor for the correction.

2.5 NGLAO Opto-Mechanics

The opto-mechanics for the NGLAO option comprise four X-Y stages each patrolling one quadrant out to 10' radius. A pickoff mirror directs the light to a Shack-Hartmann WFS camera with subapertures approximately 1-2 m, determined by the final performance predictions, the currently selected cameras are CCD-220 based systems, to maximize sensitivity. The patrol units are envisioned to be similar to what is required for 3 tip-tilt assemblies used for the LGLAO option.

The pick off mirrors for the patrol units would likely be near the bottom surface of the instrument platform. At this height they would vignette approximately 50" FoV. Because of this vignetting it may be preferable to limit them to outside the FoV, for the simulation below we assume the patrol units to be limited to be outside of $r=6'$, this is a conservative estimate, in order to have not any impact at all on the 9.2' FoV.

2.6 NGLAO Technical Challenges

As described in the simulation section below, to achieve full sky coverage we anticipate using guide stars down to $R=17.5$, this will require using high-performance photon-counting detectors. Demonstration of these devices for WFS on telescopes prior to their deployment at the GMT is therefore necessary.

The NGLAO option has the potential for being more affected by a thick ground-layer than the LGLAO option because the natural reference stars are selected further from the center of the field (due to the dichroic this is not a problem for the LGLAO system), the potential trade-off for this performance in the presence of a thick ground-layer, is choosing

reference stars closer to the center of the field and vignetting the science field, this solution however will likely limit the sky coverage of the system.

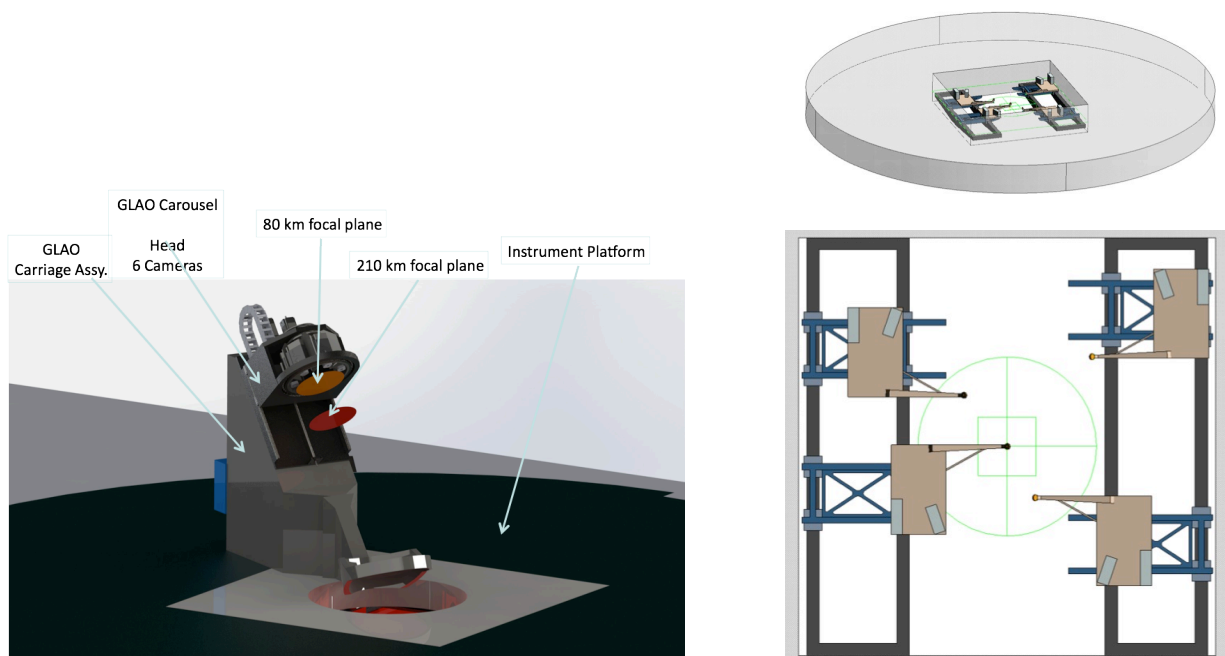


Figure 2. (Left) Mechanical Layout of the LGLAO system. (Right) Mechanical layout of the NGLAO system. Note that the LGLAO system will also need the same patrolling units for tip-tilt sensing as the NGLAO system.

3. GLAO PERFORMANCE SIMULATIONS

The key trade comparison for deciding between the LGLAO and NGLAO is the performance of each approach relative to the native seeing of the LCO site. We first describe the expected atmospheric parameters for LCO and then report the performance comparisons between the NGLAO and LGLAO options.

3.1 Expected Atmospheric Parameters

Site monitoring of LCO was carried out by Goodwin et al.² in two campaigns: September 2007, and January 2008 using a SLODAR setup first tested at Siding Springs Observatory, and moved the 100 inch Dupont telescope for the presented results. The measurements show significant differences between the campaigns. In brief, the measurements show a range of contribution from the ground layer from 20-55% of the total turbulence strengths. Goodwin et al. compiled a data set of turbulence strengths vs. height at 7 discrete heights for each campaign. By constructing “good”, “typical” and “bad” profiles for the free atmosphere (layers at 1.25, 4, 8, and 13 km) and the ground layer (layers at 25 and 400 m), they create nine distinct atmospheric models for each measurement set. We use the typical-typical set from Run 1 for detailed simulations of performance.

The “GMT Site Testing at Las Campanas Observatory”, by Thomas-Osip et al.³ provides detailed information on the ground-layer and overall site characteristics. We describe here the measurements that inform the expected performance of the GLAOS, and potential differences between the NGLAO and LGLAO options. The median fractional power in the ground layer (<500 m) is measured to be 66%, based on three years of MASS-DIMM measurements on Campanas peak. Based on the statistics compiled for the free atmosphere, and the ground layer, the most common occurrence is a free atmosphere seeing values of ~0.2”, and a ground-layer seeing of 0.35” (Figure 40 in Thomas-Osip et al.³), while the median values are 0.45” and 0.38” respectively (Table 17 in Thomas-Osip et al.³).

A key measurement from the LCO site testing is the time constant (τ_0) for the free atmosphere and the ground layer. While the median time constant for the total atmosphere is 2.6 ms, the ground-layer time constant is 17.7 ms, this difference is significant for specifying the loop speed of the GLAO system. While diffraction-limited AO might require

loop speeds of >350 Hz for typical conditions, the GLAO system could provide good correction at a much slower loop speed of approximately >100 Hz.

3.2 Sky Coverage for the NGLAO option

From the expected throughput of an NGLAO WFS and the atmospheric statistics above, we expect the limiting magnitude of usable stars to be $r=17.5$. We evaluated 100 star fields using the SDSS catalog, within 10 degrees of the north galactic pole to estimate the availability of asterism for NGLAO. We use an annulus of $r=6-8$ arcminutes for the patrol field, and require symmetry in the asterism. Figures 3-5 show the various parameters of the resulting fields.

The median number of stars in the patrol annulus is 12 stars at the galactic pole (Figure 3). This gives significant redundancy to select a reasonable asterism. All cases have more than the minimum of 3-4 guide stars in the patrol field.

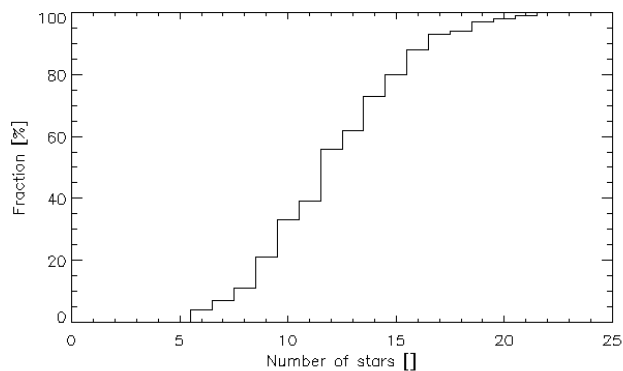


Figure 3 Distribution of the number of stars in a $r=6-8'$ annulus at the galactic pole with $r<17.5$. The median is 12, with all cases having more than 5 stars.

The median distance the stars are away from the science field is $r=6.9'$ (Figure 4, left). This is an artifact of the patrol field being defined at $r=6-8'$. Based on the stellar density (0.14 stars/sq. arcmin for $r<17.5$) there would be a 50% chance of finding an asterism at $r=4'$ even at the galactic pole. This suggests, that while the NGLAO asterism will, in general, have a larger size than the LGLAO option the distinction in asterism size is not dramatic.

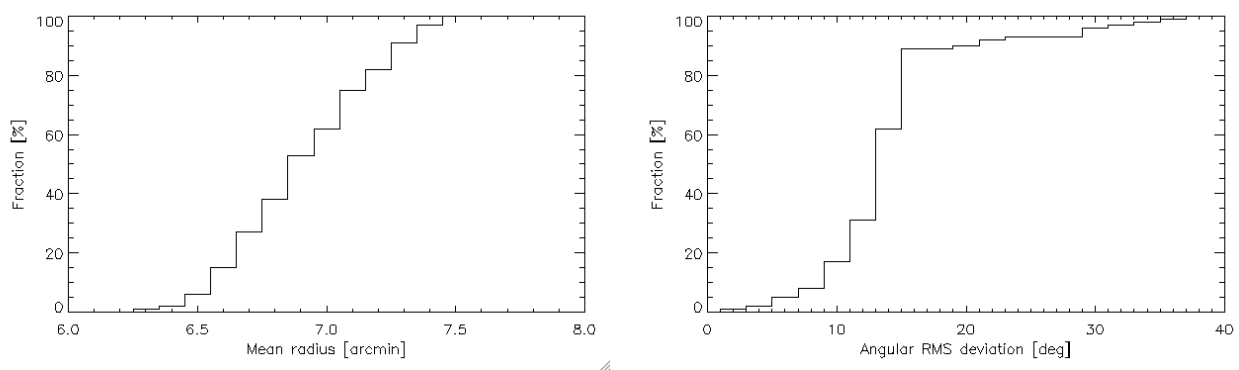


Figure 4 Distribution of the mean radius of stars forming an asterism (left). Since the asterism is constrained to be selected from a patrol field of $6-8'$ the median value of $6.9'$ is larger than an unconstrained value would be. (Right) RMS deviation of the NGLAO asterism from a square. About 90% of the asterisms are within an angular RMS deviation of 15 degrees from a perfect square.

We prefer to have asterisms that are in a square of 4 stars. Figure 4 (right) shows the typical deviation of that asterism from a perfect square. Approximately 90% of the cases have an RMS deviation of <15 degrees to the azimuthal variation of each star from a square. The range of brightness in an asterism is useful for understanding how close to the photon noise limit we will need to operate. For the patrol field chosen (annulus= $6-8'$) guide stars are typically $r=13-16$, well above the noise limit (Figure 5).

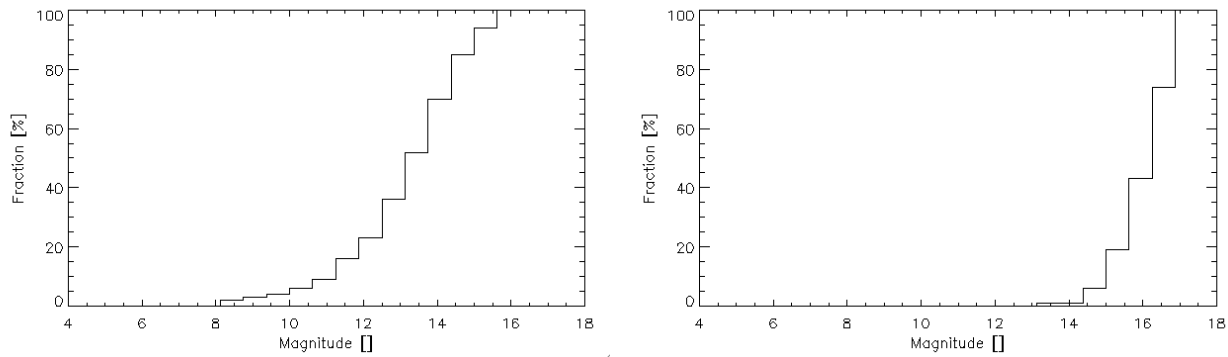


Figure 2 Distribution of the brightest guide star (left) and the faintest guide star (right) in an asterism at the galactic pole. Bright guide stars tend to have a magnitude of $r=13$, with 95% $r<15$. Even the faintest guide stars tend to be $r=16$ in an asterism.

3.3 Simulation Parameters

The simulations performed are based on an original code built to evaluate multi-conjugate adaptive optics performances for 8-m class telescope (see Brusa et al.⁴). The original code computed 'optimal' modal tomography performances and used a modal (Zernike) representation of meta-pupils together with an open loop maximum a posteriori (MAP) reconstruction technique (see, for instance, references⁵⁻⁷). To mimic a Ground Layer Adaptive Optics (GLAO) mode the code was revised to include an estimate of the average wavefront for a regular asterism of reference stars at a given polar angle (called hereafter GLAO polar angle). Additional code was written to allow the selection of natural reference star asterisms for a given direction in the sky. The selection criterion is based on statistical analysis of the available sky asterisms reported by the Sloan Digital Sky Survey (SDSS) online catalog.

The main purpose of the simulations is to determine GLAO performances in the presence of limited reference star flux (natural guide stars) and irregular reference star asterism, to compare the NGS-only based system with an LGS plus NGS tip-tilt stars systems. The code was validated against the code provided by Tokovinin⁸ in a case of high star flux and regular star geometry.

The main characteristics of the simulation are:

1. Ideal' tip-tilt wavefront sensing over sub-apertures.
2. Additive noise based on sub-aperture size, seeing value and photon flux.
3. Reconstruction based on prior turbulence profile knowledge.
4. Open loop MAP reconstruction.

The simulation does not take into account: specific WFS characteristics like aliasing or centroiding errors, effect of closed loop operation, i.e. stability requirements and detailed error rejection function, effect of partial turbulence profile knowledge.

The simulation input parameters are: telescope diameter, number of sub-apertures, turbulence heights and strengths, science field dimensions, the science observing wavelength and GLAO reference asterisms polar angle.

The simulation produces a map (over the science field) of the covariance matrix of the Zernike modes decomposition of the residual phase error at the observing wavelength. Using the covariance matrix the point spread function (PSF) at discrete point in the field and for the observing wavelength are computed from which peak intensities, FWHM and encircled energy functions can be derived.

The reconstruction process is truncated to a maximum number of modes (or radial order) on the telescope entrance pupil to keep the size of the problem tractable, in general this is not enough to produce an exact estimate of the partially corrected PSF, therefore further, not compensated, higher order polynomials are introduced for the computation of the corrected PSF.

3.4 GLAO Simulation Case

The simulation case compares the two systems introduced above: an NGS only GLAO (NGLAO) and an NGS plus LGS case (LGLAO), the aim of the study is to compare performances to provide input for the selection of the type of GLAO

system to be used by the Giant Magellan Telescope (GMT). For both cases the same (up to 50) number of randomly chosen targets was selected and in particular, to address the sky coverage issue present for the NGLAO system, we decided to limit the targets to a galactic latitude > 80 deg.

The simulation used a circular aperture of 25.4m and tip-tilt wave-front sensor with up to 24×24 sub-apertures. The conjugate plane of the corrector (adaptive secondary) was taken into account and set to 160 meters above the telescope.

A single turbulence profile corresponding to the one reported in Goodwin² as ‘typical-typical’ and based on the September 2007 seeing measurement campaign is presented here. This profile corresponds to combining the typical free atmosphere (FA) profile measured during the campaign with the typical ground layer (GL) profile and gives ~ 0.7 arc-sec seeing (at a wavelength of $0.5 \mu\text{m}$) and approximately 50% of the turbulence strength in the GL (\sim below 600 meters). The chosen profile (see Table 1) was further modified to lump together the turbulence present at 8km and 13 km into a single layer at 8 km to improve the fidelity of the computation, this modification does not affect the total seeing or the relative contribution to the total turbulence of FA and GL terms and is not expected to significantly affect the predicted performances.

Layer height [m]	Fractional turbulence power []
25	0.4608
400	0.0772
1250	0.1787
4000	0.1141
8000	0.0694
13000	0.0999

Table 1 - Typical-typical profile extracted from Goodwin. The last two layers (8km and 13 km) were combined at 8km for the simulation case.

To compute the number of photons received per frame we assumed a 5ms integration time of the wave-front sensor which seems adequate targeting the GL which displays larger correlation times. The number of reconstructed modes was approximately matched to the number of sub-apertures (see Table 2) and to compute the corrected PSF (K-band) we introduced an uncorrected modal term to fill the gap from the corrected modes up to 1891 modes (60th radial order), this order is adequate to reproduce the seeing limited PSF FWHM to within a few percent error. Finally the guide star selection was done for each field assuming three stars for the LGLAO (in an annulus of radii 8 and 10 arc-min) and four for the NGLAO (in an annulus of radii 6 and 8 arc-min). It should be noted that for the tip-tilt stars used in the LGLAO we assumed a full SH (for simplicity) however only the tip-tilt is used in the reconstruction process, since only photon noise is considered and in the framework of the simulation this is equivalent to having a pure global tip-tilt sensor. Table 2 summarizes the parameters common to both (LGLAO and NGLAO) simulated systems. Table 3 and 4 reports the parameters specific to each one of the two systems, finally Figure 6 shows the geometry used for the simulations

Telescope diameter	25.4 m
Throughput to the WFS	0.5
Number of sub-apertures	Up to 24x24
Turbulence profile	Modified Goodwin September 2007, typical-typical (see ² and text)
Number of reconstructed Zernike modes	Up to 435 ($r_{ord} = 28$) for the 24x24 case
Total number of Zernike modes used for PSF estimation	1891 ($r_{ord} = 60$)
Science field	7 arc-min x 7 arc-min (square)
Science observing band	K-band
Reference GLAO radius	4.5 arc-min

Table 2 - Parameters for the simulation common to both LGLAO and NGLAO case.

NGS inner search radius	6 arc-min
NGS outer search radius	8 arc-min
NGS max R magnitude	17.5 ($= 10^3 \text{ ph s}^{-1} \text{ m}^{-2}$)
Maximum number of NGS stars	4

Table 3 - Parameters specific to the NGLAO case.

NGS inner search radius	8 arc-min
NGS outer search radius	10 arc-min
NGS max R magnitude	17.5
Maximum number of NGS stars	3
Number of LGS	6 (hexagon)
LGS radius	3.5 arc-min
LGS flux	$10^7 \text{ ph s}^{-1} \text{ m}^{-2}$
LGS angular size	1 arcsec

Table 4 - Parameters specific to the LGLAO case.

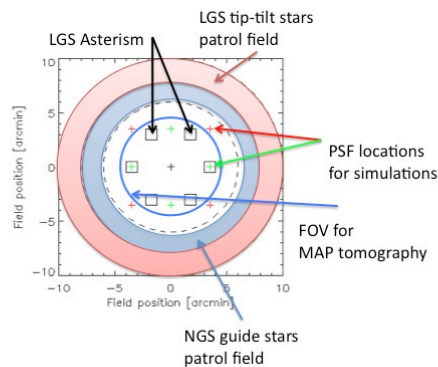


Figure 6 Map of the science field, with locations of the PSFs samples points (crosses in black, green and red). The blue annulus ($r=6-8'$) marks the NGLAO patrol field. The red annulus ($r=8-10'$) shows the patrol field for the LGLAO tip-tilt stars. The LGS asterism is shown with black squares while the GLAO polar angle is shown by the solid line circle (blue).

3.5 Simulation results

To estimate the performances we computed FWHM of corrected PSF in the science field as a function of the number of sub-apertures used to sample the entrance pupil of the telescope. For the case considered it was found that the NGLAO performances saturate at about 18x18 sub-apertures, as can be seen in Figure 7, and that some improvement is possible beyond 24x24 sub-apertures (see Figure 8) for the LGLAO system.

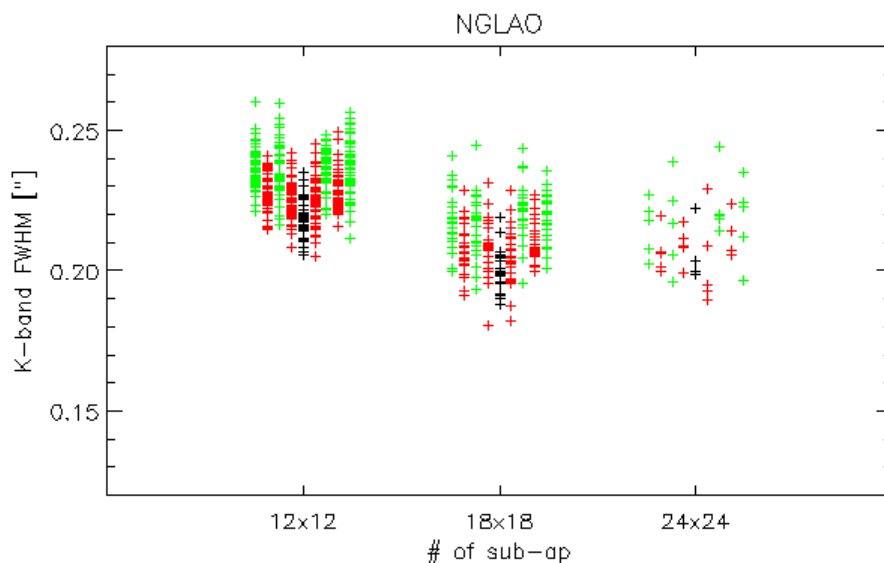


Figure 7 Computed performances for the NGLAO case as a function of the number of sub-apertures. The black, green and red crosses correspond to the field points shown in Figure 6

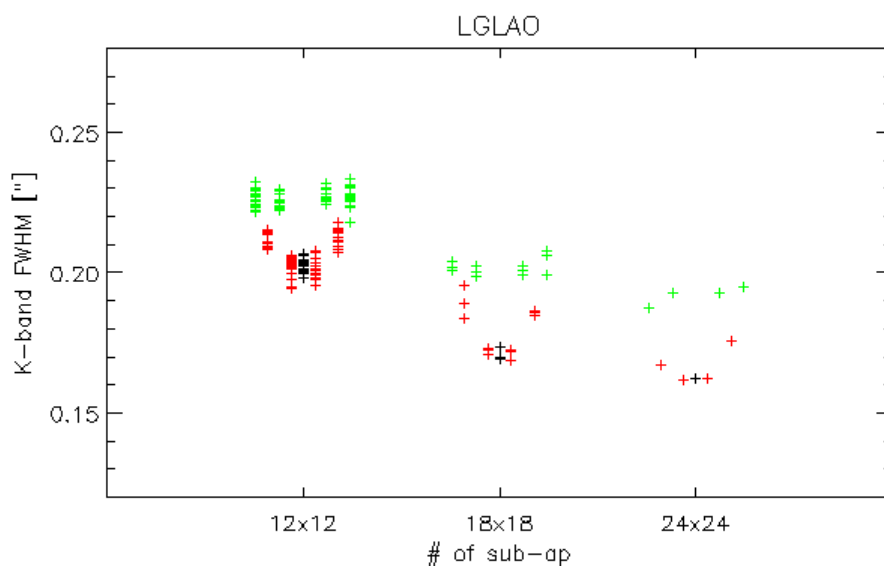


Figure 8 Computed performances for the LGLAO case as a function of the number of sub-apertures. The black, green and red crosses correspond to the field points shown in Figure 6.

FWHM of the corrected K-band PSFs are shown for the 24x24 sub-aperture case in Table 5. The reported values are for nine points in the field: the center of the field, four points in a cross pattern on the edges of the field (3.5 arc-min radius) and four other points at the corners of the field (~5 arc-min radius), as shown in Figure 6.

A reduction of the FWHM (K-band) by a factor of 2-2.5 with respect to the seeing limited images (nominally with a FWHM of 0.51") is produced by both systems. The comparison shows that the LGLAO system produces somewhat better performances with FWHMs about 10-20% smaller; the LGLAO also produces less variability of the FWHMs across target samples as reported by the standard deviation. We also point out that the LGLAO system does not produce a completely axisymmetric distribution of the FWHM, apparent consequence of the hexagonal pattern of the LGS asterism.

0.215" \pm 0.010" (0.192" \pm 0.003")	0.207" \pm 0.008" (0.181" \pm 0.003")	0.216" \pm 0.017" (0.192" \pm 0.002")
0.209" \pm 0.007" (0.167" \pm 0.004")	0.204" \pm 0.010" (0.160" \pm 0.002")	0.203" \pm 0.016" (0.169" \pm 0.004")
0.223" \pm 0.012" (0.195" \pm 0.002")	0.211" \pm 0.008" (0.178" \pm 0.003")	0.218" \pm 0.014" (0.192" \pm 0.004")

Table 5 - Computed FWHM for NGLAO (black) and LGLAO (red and in parenthesis) cases for 24x24 sub-apertures. The nine points correspond to the nine locations in the science field shown in Figure 6. Only one asterism was used for the LGLAO case, we therefore report here the standard deviation, for the 12x12 case for which enough statistics was computed. Notice that the lack of azimuthal symmetry in the FWHM for the LGLAO case is reflecting the alignment of the hexagonal pattern of LGS.

3.6 Simulations Results Discussion

As shown in the previous paragraph it appears that the NGLAO produces somewhat lower performances than the LGLAO one, this is to be expected given the much more favorable configuration for the LGLAO system. It is interesting to notice however that the NGLAO system is able to meet the GLAO requirements (see Introduction and reference ¹) while as already pointed out, is significantly less complex than the LGLAO system.

Two more points should be mentioned here, first: the absolute value of the corrected PSF's FWHM is very much dependent on the fraction of power present in the GL as well as its exact distribution within this region, we are planning therefore to run further cases enough turbulence profiles to reproduce a significant fraction of the observing nights. Secondly, although the requirement is in term of corrected PSF's FWHM it is worth noting that the FWHM improvement, i.e. FWHM(s.l.)/FWHM(GLAO) should be computed using the correct outer scale, in this case, for instance assuming a 60m outer scale the expected FWHM(s.l.) \sim 0.37" vs. 0.51" for an infinite outer scale case, i.e. the uncorrected FWHM is significantly smaller and therefore the corresponding FWHM improvement.

3.7 Future simulation activity

Our future simulation activity will be directed in three main directions:

1. Evaluate the variability of the performances with using more more measured profiles at Cerro Las Campanas.
2. Assess the sensitivity of the results on turbulent layers distribution 'a priori' knowledge and corresponding requirement on this knowledge.
3. Evaluate the expected performances with a more detailed simulation code that includes both sensor specific characteristic as well as closed loop operation: at the moment the YAO software, with appropriate modifications, is being considered.

4. SCOPE COMPARISON OF NGLAO AND LGAO

In addition to performance, the scope and complexity of the two concepts are factors that may influence the final approach taken for the GMT project. There is a significant increase in scope and complexity for the LGLAO system, compared to the NGLAO system. In particular the LGLAO system has:

- A large dichroic (0.6-0.8 m) that must be deployed and retracted.
- Sodium lasers and a beam projector that, while shared with the LTAO system, needs to project a wide asterism,
- Additional interfaces with the beam projector, the patrolling units, and the WFS stage.

In addition to an increased scope, the larger number of subsystems for the LGLAO system makes it naturally more susceptible to loss of efficiency via a failure of a subsystem. We expect the key areas of failure for the LGLAO system to be that of a laser beacon, or a loss of a patrolling tip-tilt stage. Similarly, we expect the NGLAO system to be mainly affected by the loss of one patrolling WFS.

The NGLAO system provides more versatility than the LGLAO system. It can more easily be operated to cover a range of field sizes, simply by choosing an asterism that encloses the desired field size. The system can operate without any additional optics in the beam, allowing more routine functioning over a range of wavelengths, and with any instrument designed for seeing-limited operation. Finally, the use of natural guide stars, by its nature is its own truth sensor, negating any need for sodium layer monitoring.

The NGLAO option benefits from lower design and fabrication costs, as well as a shorter development time. It is also dependent on fewer subsystems to perform to its requirements. These several functional differences make the NGLAO an attractive option. On the other hand, small fields-of-view (2-4') may benefit from the likely improved and consistent image improvement of an LGLAO system.

5. AN OVERALL COMPARISON OF NGLAO AND LGLAO

The various comparisons described above can be captured by numerical ratings of the various preferences; this section attempts to assign weights and grades to all of the criteria described above, in order to trace the preference for one option over the other. While the weights, and to some extent, the grades are subjective they are useful as a quick summary of the topics and relative merits for comparison. The next section reports the metric categories and Table 6 summarizes the results of the trade study.

5.1 Metric Categories

Performance in support of AO is the concept's ability to meet and exceed AO requirements. Both concepts are designed to meet the science requirements. The higher rating given to the LGLAO option is due to its expected improved performance for smaller sub-apertures and over smaller field sizes.

Performance in support of science. This category is intended to capture the impact of operating the GLAOS on scientific instruments. Throughput and efficiency of operation are likely to be impacted for the LGLAO option. Field distortion and emissivity may also impact science instrument performance for the LGLAO system. The NGLAO option would likely be nearly invisible to the science instrument, giving it the preference in this category. The NGLAO can also deliver a larger field to the instrument.

Software: The metric used to estimate complexity is lines of code or modules and the rating reflects NGLAO is expected to have 1/3 less than LGLAO. The additional subsystems in LGLAO decrease its rating.

Optics: The dichroic concept is at the maximum size obtainable from a vendor with suitable figure, coating and stability in mount. This may be a risk item. The NGLAO WFS optical components are routine.

Electro-Mechanics: The LGLAO has additional moving precision components.

Systems Eng. (Interfaces): Both systems interface to the instrument platform. Both interface to the AO RTC wavefront processor. The LGLAO option also interfaces to the laser system and has a separate subsystem on the top of the instrument platform, and the dichroic deployment mechanism. The laser system is a single point failure for LGLAO.

Cost: The cost is expected to be nearly double for the LGLAO option. The cost uncertainty is higher.

Schedule: The NGLAO option can be developed and deployed in a shorter time.

Schedule Risk: For LGLAO, prototyping of the camera head carousel may be needed. The NGS WFS are more standard systems. Getting the LGLAO system online is tied to laser system development schedule.

CRITERIA	WEI GHT %	Rating Scale	NGLAOS Rating	NGLAOS Weight x Rating	LGLAOS Rating	LGLAOS Weight x Rating
Performance	25	Most supportive to AO =3 Least Supportive =1	2	50	2.5	62.5
Performance	25	Most support. Science =3 Least Supportive =1	3	75	2	50
Tech. Complexity						
Software	7.5	Least Challenging = 3 Most Challenging=1	2.5	18.75	2	15
Optics	7.5	Least Challenging = 3 Most Challenging=1	3	22.5	1	7.5
Electro- Mechanics	5	Least Challenging = 3 Most Challenging=1	3	15	2	10
Systems Eng. (Interfaces)	7.5	Least Challenging = 3 Most Challenging=1	3	22.5	2	15
Fault Tolerance	5	Most tolerant=3 Least tolerant=1	3	15	2	10
Cost	12.5	Least Expensive = 3 Most Expensive = 1	3	37.5	1	12.5
Schedule	2.5	Shortest Development = 3 Longest Development = 1	2	5	1	2.5
Schedule Risk	2.5	Least Uncertainty = 3 Most Uncertainty = 1	2	5	1	2.5
				266.25		187.5
Weighted Totals	100 %	3		89%		63%

Table 6. Trade Study Comparison Matrix. The yellow shaded boxes are areas of concern for each option.

6. CONCLUSIONS

The NGLAO and LGLAO options have complementary strengths for the GMT. It is clear that the ultimate performance for a given field is provided by the LGLAO, but at a significant increase in complexity and potentially lower efficiency. The tomographic reconstruction of the atmospheric layers appears to compensate somewhat for the typically wider asterisms of the NGLAO system making the natural guide star approach an attractive option depending on the desired size of the corrected field of view.

ACKNOWLEDGMENTS

This work has been supported by the GMTO Corporation, a non-profit organization operated on behalf of an international consortium of universities and institutions: Astronomy Australia Ltd, the Australian National University, the Carnegie Institution for Science, Harvard University, the Korea Astronomy and Space Science Institute, the Smithsonian Institution, The University of Texas at Austin, Texas A&M University, University of Arizona and University of Chicago. This material is based in part upon work supported by AURA through the National Science Foundation under Scientific Program Order No. 10 as issued for support of the Giant Segmented Mirror Telescope for the United States Astronomical Community, in accordance with Proposal No. AST-0443999 submitted by AURA.

REFERENCES

- [1] Bouchez A. H. et.al., "The Giant Magellan Telescope Adaptive Optics Program", Proc. SPIE 8447-54 (this conference), (2012).
- [2] Goodwin, M, "Turbulence profiling at Siding Springs and Las Campanas Observatories", PhD Thesis, The Australian National University, 2009;
- [3] Joanna Thomas-Osip, Matt Johns, Pat McCarthy, Mark M. Phillips, and Gabriel Prieto GMT-SE-DOC-00114, GMT "GMT Site Testing at Las Campanas Observatory Final Report".
- [4] Brusa G., Riccardi A., Esposito S., Femenia B. and Carbillet M., "Multiconjugate AO system for 8-m class telescopes", Proc. SPIE 4034, pp. 190-200 (2000);
- [5] Ragazzoni R., Marchetti E. and Rigaut F., "Modal tomography for adaptive optics", A&A, Vol. 342, L53-L56 (1999);
- [6] Johnston, D. C. and Welsh, B. M., "Analysis of multiconjugate adaptive optics", JOSA A, Vol. 11, pp. 394-408 (1994);
- [7] Tokovinin A., Le Louarn M., Viard E., Hubin N., Conan R., "Optimized modal tomography in adaptive optics", A&A, Vol. 378, pp. 710-721 (2001);
- [8] Tokovinin A., "Seeing Improvement with Ground-Layer Adaptive Optics", PASP, Vol. 116, pp. 941-951, (2004);